

A Pyridine-Containing Anthracene Derivative with High Electron and Hole Mobilities for Highly Efficient and Stable Fluorescent Organic Light-Emitting Diodes

Yongduo Sun, Lian Duan, Deqiang Zhang, Juan Qiao, Guifang Dong, Liduo Wang, and Yong Qiu*

A pyridine-containing anthracene derivative, 9,10-bis(3-(pyridin-3-yl)phenyl)anthracene (DPyPA), which comprehensively outperforms the widely used electron-transport material (ETM), tris(8-quinolinolato) aluminum (Alq₃), is synthesized. DPyPA exhibits ambipolar transport properties, with both electron and hole mobilities of around $10^{-3} \text{ cm}^{-2} \text{ V}^{-1} \text{ s}^{-1}$; about two orders of magnitude higher than that of Alq₃. The nitrogen atom in the pyridine ring of DPyPA coordinates to lithium cations, which leads to efficient electron injection when LiF/Al is used as the cathode. Electrochemical measurements demonstrate that both the cations and anions of DPyPA are stable, which may improve the stability of devices based on DPyPA. Red-emitting, green-emitting, and blue-emitting fluorescent organic light emitting diodes with DPyPA as the ETM display lower turn-on voltages, higher efficiencies, and stronger luminance than the devices with Alq₃ as the ETM. The power efficiencies of the devices based on DPyPA are greater by 80–140% relative to those of the Alq₃-based devices. The improved performance of these devices is attributed to the increased carrier balance. In addition, the device employing DPyPA as the ETM possesses excellent stability: the half-life of the DPyPA-based device is 67 000 h—seven times longer than that of the Alq₃-based device—for an initial luminance of 5000 cd m⁻².

1. Introduction

Organic light-emitting diodes (OLEDs) have attracted a great deal of attention due to their potential applications in full-color flat-panel displays and illumination.^[1] The charge balance in OLEDs is considered to be essential for achieving high performance. Many high-mobility hole-transport materials (HTMs) have been designed and synthesized.^[2] However, electron-transport materials (ETMs) with high mobility are relatively rare.^[3] The most widely used ETM is still tris(8-quinolinolato)

aluminum (Alq₃), although it possesses low electron mobility, and the instability of cationic Alq₃ is considered to be responsible for OLED degradation.^[4] Thus, developing high-performance ETMs with high electron mobility and good stability is crucially important for improving OLED performance.^[3] To improve the electron mobility of organic semiconductors, aza-aromatics such as phenanthroline, quinoline, pyridine, and triazole have been incorporated into π -conjugated systems.^[5] However, OLEDs that use aza-aromatics as ETMs usually show short lifetimes.^[5] In this paper, we report the synthesis and investigation of a new anthracene-based compound: 9,10-bis(3-(pyridin-3-yl)phenyl)anthracene (DPyPA), which incorporates 3-(pyridin-3-yl)phenyl—an outstanding electron-transport chromophore^[5b]—as the substituent. DPyPA was found to possess high electron mobility (around $10^{-3} \text{ cm}^2 \text{ V}^{-1} \text{ s}^{-1}$) and easy injection of electrons from the cathode as well as appropriate highest occupied molecular orbital (HOMO) and lowest unoccupied

molecular orbital (LUMO) energy levels. Furthermore, cyclic voltammetry (CV) measurements reveal that both the cations and anions of DPyPA are stable, which may lead to improved device stability. Red-emitting, green-emitting, and blue-emitting devices that employ DPyPA as the ETM exhibit lower turn-on voltages, higher efficiencies, and larger luminances than the devices with Alq₃ as the ETM. In addition, the OLED employing DPyPA as the ETM also possesses better stability than the Alq₃-based device, which indicates that it is possible to create materials containing aza-aromatics as ETMs that can form OLEDs with both high performance and good stability.

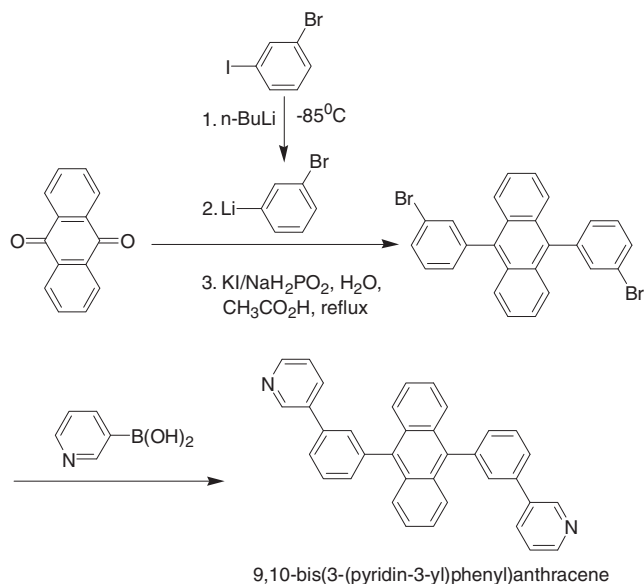
2. Results and Discussion

2.1. Synthesis and Characterization

Scheme 1 illustrates the synthetic approach to DPyPA. Anthraquinone reacted with (3-bromophenyl) lithium, which was synthesized from 3-bromo-iodobenzene and

Y. Sun, Dr. L. Duan, D. Zhang, Dr. J. Qiao, Prof. G. Dong, Prof. L. Wang, Prof. Y. Qiu
Key Lab of Organic Optoelectronics and Molecular Engineering
of Ministry of Education
Department of Chemistry
Tsinghua University
Beijing 100084, PR China
E-mail: qiyu@mail.tsinghua.edu.cn

DOI: 10.1002/adfm.201002691



Scheme 1. Synthetic routes of DPyPA

n-butyllithium, to form 9,10-bis(3-bromophenyl)anthracene. Then, 9,10-bis(3-bromophenyl)anthracene reacted with pyridin-3-ylboronic acid via a palladium-catalyzed Suzuki coupling reaction to form the desired product, 9,10-bis(3-(pyridin-3-yl)phenyl)anthracene (DPyPA).^[6] The structure of DPyPA was confirmed by mass spectrometry, elemental analysis, ¹H NMR, and ¹³C NMR. All materials used in the devices were purified by repeated temperature-gradient vacuum sublimation.

2.2. Thermal and Photophysical Properties

The thermal properties of DPyPA were determined by differential scanning calorimetry (DSC) and thermogravimetric analysis (TGA). DPyPA has a glass-transition temperature (T_g) of 97 °C, a melting temperature (T_m) of 268 °C, and a decomposition temperature (T_d , corresponding to 5% weight loss) of 442 °C. The absorption spectra and photoluminescence (PL) spectra of DPyPA in CH₂Cl₂ (2×10^{-4} M) and the vacuum-evaporated DPyPA film on the quartz substrate are shown in **Figure 1**. The absorption spectra of DPyPA in the solution and solid state exhibit peaks at 375 nm and 381 nm, respectively, which can be attributed to π - π^* transitions. The solution-PL emission peak occurs at 432 nm, while the thin-film PL emission is around 443 nm.

2.3. Electrochemical Properties

The electrochemical properties of DPyPA were studied by CV. As shown in **Figure 2**, one quasireversible oxidation potential occurs at 1.50 V and one reversible reduction potential at -1.68 V, which indicates that both the radical cations and anions are stable entities.^[7a] The HOMO of DPyPA is 5.9 eV, which was determined from the anodic oxidation potential by

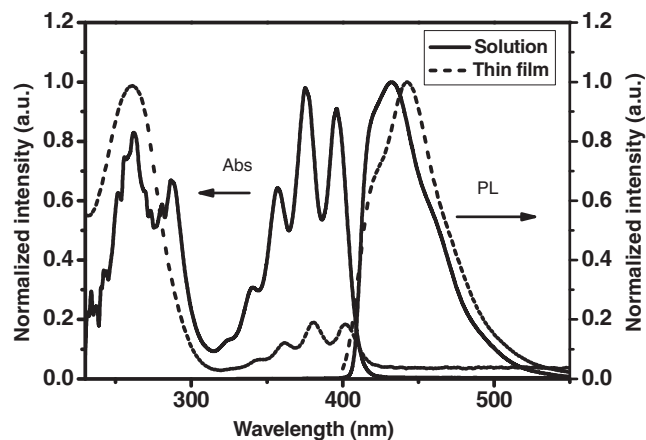


Figure 1. Absorption and PL-emission spectra of CH₂Cl₂ solution and thermally evaporated film of DPyPA.

using the previously reported HOMO of ferrocene (4.8 eV) as a reference.^[7b] The LUMO was calculated from the HOMO value and the energy gap (E_g) from the edge of the absorption spectrum to be about 2.8 eV.^[7c] For Alq₃ under identical experimental conditions, however, both the oxidation potential and reduction potential are irreversible. And the HOMO and LUMO of Alq₃ are 5.7 eV and 3.0 eV, respectively.

2.4. Carrier-Transport Properties

The carrier mobilities of the DPyPA thin film were characterized by the time-of-flight (TOF) transient-photocurrent technique.^[8] The configuration of the device is ITO/Ag (60 nm)/organic layer (1.4 μ m)/Ag (200 nm). The carrier mobility (μ) was calculated from the values of the transit time (T_t),

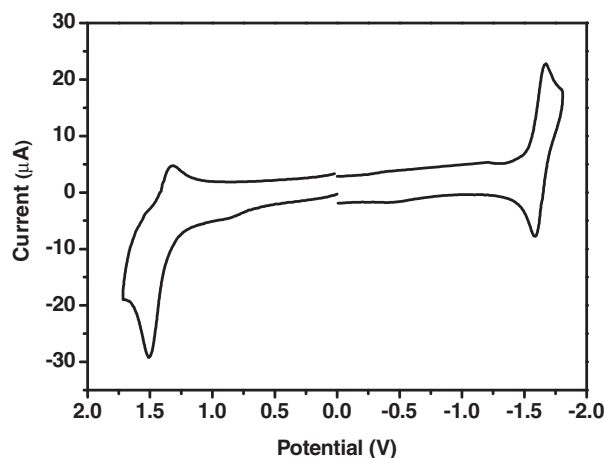


Figure 2. CV of DPyPA. Working electrode: Pt disc; reference electrode: Ag/AgCl. Oxidation CV was performed in dichloromethane containing 0.1 M *n*-Bu₄NCl₆ as the supporting electrolyte at a scan rate of 300 mV s⁻¹. Reduction CV was performed in *N,N*-dimethyl formamide (DMF) with 0.1 M *n*-Bu₄NClO₄ as the supporting electrolyte at a scan rate of 200 mV s⁻¹.

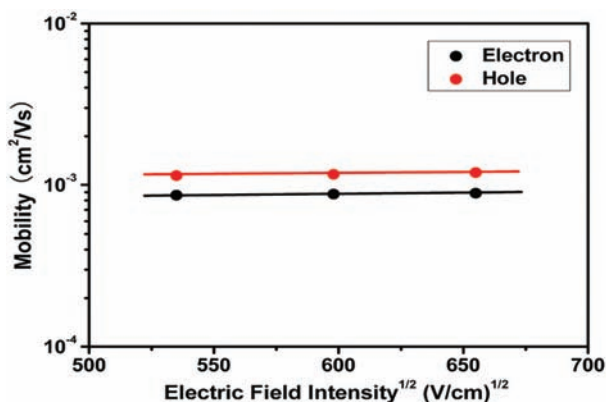


Figure 3. Electron and hole mobilities of DPyPA film plotted as a function of the square root of the electric field.

the sample thickness (D) and the applied voltage (V) by using the following equation: $\mu = D^2/(VT_i)$. As shown in **Figure 3**, DPyPA displays high electron mobility (around $1 \times 10^{-3} \text{ cm}^2 \text{ V}^{-1} \text{ s}^{-1}$) at an electric field of $4 \times 10^5 \text{ V cm}^{-1}$, which is comparable to the highest reported electron mobility,^[5b] and is about two orders of magnitude higher than that of Alq₃.^[9] DPyPA also exhibits high hole mobility that is close to the electron mobility.

To verify the ambipolar nature of DPyPA, we fabricated a single-layer device with a structure of ITO/MoO₃ (2 nm)/DPyPA (100 nm)/Mg: Ag (150 nm)/Ag (50 nm). MoO₃ was used as the hole-injection layer. This device emitted a deep blue light that comes from DPyPA itself. The device produced a maximum current efficiency of 0.9 cd A^{-1} , a maximum brightness of 3301 cd m^{-2} , and a turn-on voltage of 4.8 V. The results demonstrate that DPyPA is capable of functioning as both electron-transport and hole-transport material. The electroluminescence (EL) emission spectrum and typical current density–luminance–voltage (J – L – V) characteristics of the single-layer device are shown in the Supporting Information (SI).

2.5. Quantum Chemical Calculations

Theoretical calculations on the electronic states of DPyPA were carried out at the DFT//B3LYP/6-31G level in the Gaussian 03 program^[10] to acquire a better understanding of the ambipolar properties. As shown in **Figure 4**, both HOMO and LUMO are mainly located on the anthracene core in DPyPA, which results in similar charge-transfer integrals for electrons and holes. According to Marcus theory, similar charge-transfer integrals for electrons and holes will lead to balanced electron- and hole-transport properties,^[11] so the ambipolar transport properties of DPyPA may result from the overlap of frontier orbitals on the anthracene core. This agrees well with our previous work, in which several naphtho[2,3-*c*][1,2,5]thiadiazole derivatives exhibited ambipolar transport properties because of the similar charge-transfer integrals for electrons and holes.^[12]

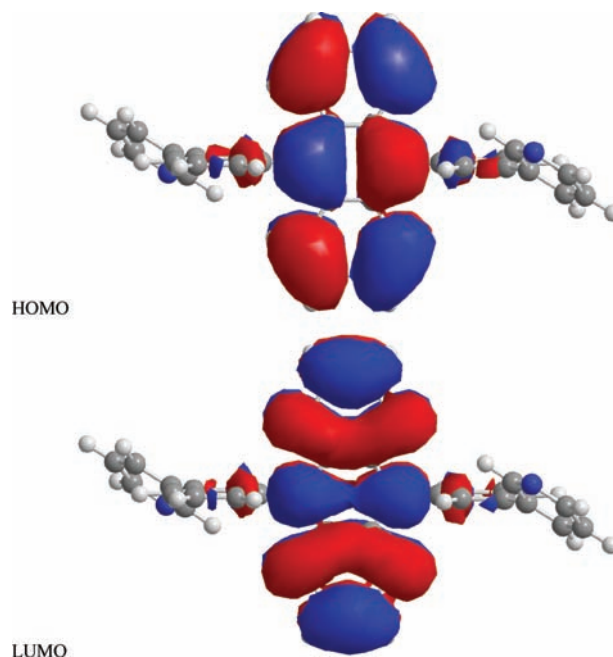


Figure 4. The molecular-orbital surfaces of HOMO and LUMO of DPyPA calculated at the DFT//B3LYP/6-31G level.

2.6. Electroluminescent Properties

To evaluate the possible applications of DPyPA in OLEDs, red, green, and blue OLEDs were fabricated with DPyPA as the ETM. Devices with Alq₃, the most widely used ETM, were also fabricated for comparison. The structures of the devices were as listed below, where NPB is 4,4'-N,N'-bis[N-(1-naphthyl)-N-phenylamino]biphenyl, DNTPD is N,N'-di(4-(N,N'-diphenyl-amino)phenyl)-N,N'-diphenylbenzidine, DTDP is dibenzo([f,f']-4,4',7,7'-tetraphenyl)diindeno(1,2,3-cd:1',2',3'-lm)perylene, F4TCNQ is 2,2'-(perfluorocyclohexa-2,5-diene-1,4-diyldiene)dimalononitrile, ADN is 9,10-di(naphthalen-2-yl)anthracene, PADN is 9,10-di(naphthalen-2-yl)-2-phenylanthracene, DPAVBi is 4,4'-(1E,1'E)-2,2'-(biphenyl-4,4'-diyl)bis(ethene-2,1-diyl)bis(N,N-dip-tolylaniline), rubrene is 5,6,11,12-tetraphenyltetracene, HAT is dipyrazino[2,3-f:2',3'-h]quinoxaline-2,3,6,7,10,11-hexacarbonitrile and DTBTDD is 2,6-di-tert-butyl-N9,N9,N10,N10-tetrap-tolylanthracene-9,10-diamine.

Red device A1: ITO/4.2% F₄TCNQ-doped DNTPD (150 nm)/NPB (20 nm)/0.4% rubrene-doped ADN and DPDT (4: 6) (30 nm)/DPyPA (20 nm)/LiF (0.5 nm)/Al (150 nm).

Red device A2: ITO/4.2% F₄TCNQ-doped DNTPD (150 nm)/NPB (20 nm)/0.4% rubrene-doped ADN and DPDT (4: 6) (30 nm)/Alq₃ (20 nm)/LiF (0.5 nm)/Al (150 nm).

Green device A1: ITO/HAT (5 nm)/NPB (20 nm)/9% DTBTDD-doped PADN (30 nm)/DPyPA (20 nm)/LiF (0.5 nm)/Al (150 nm).

Green device A2: ITO/HAT (5 nm)/NPB (20 nm)/9% DTBTDD-doped PADN (30 nm)/Alq₃ (20 nm)/LiF (0.5 nm)/Al (150 nm).

Blue device C1: ITO/NPB (50 nm)/4% DPAVBi-doped ADN (30 nm)/DPyPA (30 nm)/LiF (0.5 nm)/Al (150 nm).

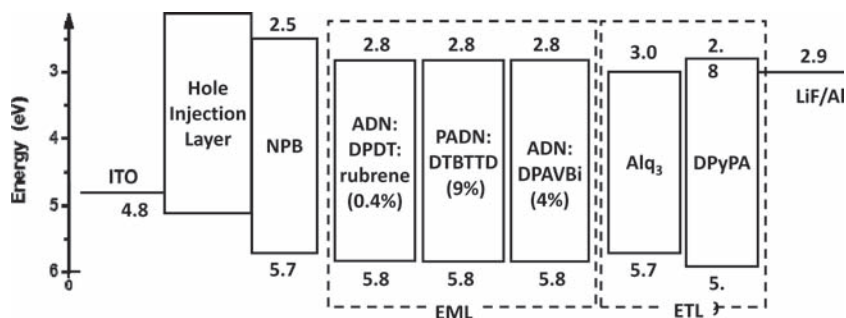


Figure 5. Energy-level diagram of the multilayer devices: HOMO and LUMO levels of DPyPA and Alq₃ were measured by CV, while those of NPB, ADN, PADN, DPDT, ITO, and LiF/Al are previously reported values.^[13]

Blue device C2: ITO/NPB (50 nm)/4% DPAVBi-doped ADN (30 nm)/Alq₃ (30 nm)/LiF (0.5 nm)/Al (150 nm).

The structures of the devices and the energy levels of the materials are shown in **Figure 5**. The LUMO level of DPyPA is near to that of Alq₃, while the HOMO level of DPyPA is 0.2 eV lower than that of Alq₃, which may act as a hole barrier. All the devices were fabricated by high-vacuum thermal evaporation.

The current density–voltage (*J*–*V*) characteristics and the luminance–voltage (*L*–*V*) characteristics are shown in **Figure 6**, and the device performances are summarized in **Table 1**. It can be seen that devices employing DPyPA as the ETM possessed lower turn-on voltages (defined as the voltage required to give a luminance of 1 cd m⁻²) and higher efficiencies and luminances than those of the devices with Alq₃ as the ETM. At 5000 cd m⁻², the driving voltages of the devices A1, A2, B1, B2, C1, and C2 are 1.7, 2.5, 2.5, 3.3, 3.4, and 5.9 V, respectively. The driving voltage at 5000 cd m⁻² decreased by 1.6, 2.9, and 4.5 V for devices A, B, and C, respectively, by using DPyPA instead of Alq₃. The power efficiencies at 5000 cd m⁻² of the devices are 3.51, 1.91, 18.32, 8.91, 11.26, and 7.63 lm W⁻¹ for devices A1, A2, B1, B2, C1, and C2, respectively. The power efficiencies increased by about 84%, 106%, and 143%, for devices A, B, and C, respectively, compared with those of the devices with Alq₃ as the ETM.

The high efficiencies of the devices based on DPyPA are attributed to the increased carrier balance, which is due to the improved electron transport and injection. The electron mobility of DPyPA is about two orders of magnitude higher than that of Alq₃, and near to that of NPB.²⁵ The LUMO level of DPyPA is near to that of Alq₃, so together with the possible effect of the coordination of the pyridine nitrogen atom to the lithium cations,^[14] efficient electron injection from the cathode into DPyPA is guaranteed. The low driving voltages of the devices with DPyPA also result from the enhanced electron transport and injection. The experimental details in the SI also demonstrate that it is easier for coordination to take place between the LiF/Al bilayer cathode and DPyPA than between LiF/Al and Alq₃.

2.7. Stability of OLEDs

For OLEDs with aza-aromatics as the ETM, the lifetime is of great concern. We therefore studied the stability of

the OLEDs. At an initial luminance of 5000 cd m⁻², devices B1 (DPyPA-based device) and B2 (Alq₃-based device) were operated at a constant current for approximately 2800 h. It can be seen from **Figure 6** that the OLED with DPyPA exhibited better stability. The extrapolated lifetimes of devices B1 and B2, at an initial luminance of 5000 cd m⁻², are about 8900 and 67100 h, respectively. Here, we used a stretched exponential decay (SED) as previously reported: $L/L_0 = \exp[-(t/\tau)^\beta]$, where L_0 is the initial luminance, L is the luminance, β and τ are fitting parameters, and t is the test time.^[15]

Although OLEDs with aza-aromatics as the ETM usually exhibit poor stability, DPyPA seems to be an exception.^[5] As shown in **Figure 2**, DPyPA exhibits one quasireversible oxidation potential and one reversible reduction potential. This indicates that both the radical cations and radical anions of DPyPA are stable.^[7,16] The stable radical cations and radical anions may be the main reason for the improved operational stability of the OLEDs made with DPyPA.

3. Conclusion

We have designed and synthesized a high-performance ETM, DPyPA. Highly efficient red-emitting, green-emitting, and blue-emitting fluorescent OLEDs were achieved by employing DPyPA as the ETM. The increased efficiency of the OLEDs with the newly developed ETM is due to the improved electron transport and injection. The excellent operational stability may be attributed to the stable radical cations and radical anions of DPyPA. The concept, presented in this paper, of designing molecules with stable cations and anions should be extended to the design of other organic charge-transport materials.

4. Experimental Section

General Experiments: ¹H-NMR and ¹³C-NMR spectra were recorded on an ECA600 NMR spectrometer with tetramethylsilane as the internal standard and CDCl₃ as solvent. Electron-impact (EI) mass spectra were recorded on a GCT-MS Micromass UK instrument. Elemental analysis was carried out on an Elementary Vario EL CHN elemental analyzer. Absorption and PL spectra were recorded with a UV-vis spectrophotometer (Agilent 8453) and a fluorospectrophotometer (Jobin Yvon, FluoroMax-3), respectively. TGA was recorded with a Netzsch simultaneous thermal analyzer (STA) system (STA 409PC) under a dry-nitrogen flow at a heating rate of 10 °C min⁻¹. Glass-transition temperatures were recorded by DSC at a heating rate of 10 °C min⁻¹ with a thermal analysis instrument (DSC 2910 modulated calorimeter). CV was performed on a Princeton Applied Research potentiostat/galvanostat model 283 voltammetric analyzer with a platinum plate as the working electrode, a silver wire as the pseudo-reference electrode, and a platinum wire as the counter electrode. Ferrocene was selected as the internal standard. The solutions were bubbled with argon for 10 min before measurements.

Computational Methodology: The geometrical and electronic properties of the DPyPA were calculated with the Gaussian 03 program

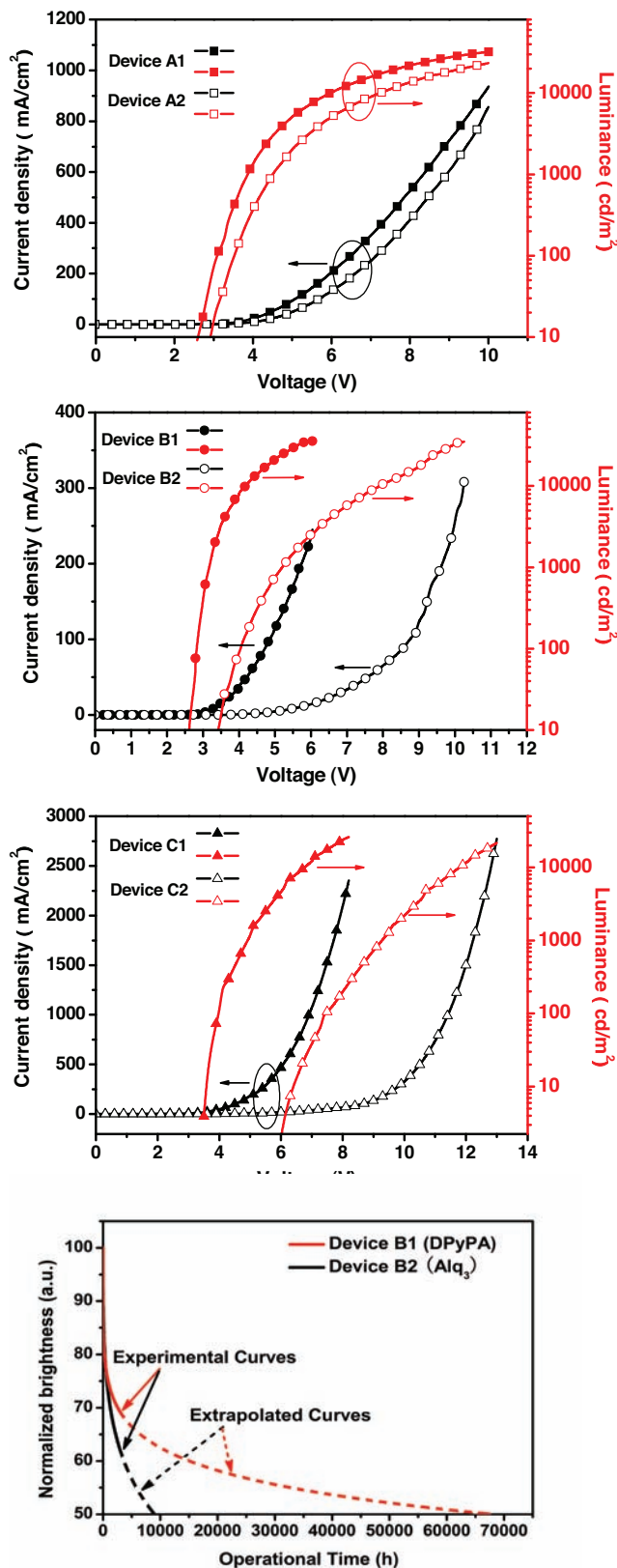


Figure 6. a–c) The current density–voltage (J – V) curves and the luminance–voltage (L – V) curves of devices A1 and A2 (red OLEDs), B1 and B2 (green OLEDs), and C1 and C2 (blue OLEDs); d) luminance–deterioration curves of devices B1 and B2 (green OLEDs).

package. The geometry was optimized by means of B3LYP with a 6-31G basis set.

Preparation of Materials: All reactants and solvents, unless otherwise stated, were purchased from commercial sources and used as received.

9,10-bis(3-bromophenyl)anthracene: *n*-butyllithium (2.9 M, 9.60 mL, 27.4 mmol) was slowly added to a solution of 3-bromo-iodobenzene (8.00 g, 28.4 mmol) in dry tetrahydrofuran (120 mL) at -85 °C under argon before anthraquinone (2.51 g, 12.0 mmol) was added all at once. The resulting mixture was stirred for 2 h, during which time the temperature rose to 20 °C. Cold water (100 mL) was added and the organic phase was isolated. The aqueous phase was extracted with ethyl acetate (2×50 mL). The combined organic fractions were dried over magnesium sulfate and the volatiles were removed in vacuo to deliver a foamy residue. To this residue were added potassium iodide (8.00 g, 48.2 mmol), sodium hypophosphite (7.62 g, 72.1 mmol), and acetic acid (100 mL), and the mixture was heated under reflux for 2 h. After cooling, the yellow precipitate was collected, washed with plenty of water, and dried. The 9,10-bis(3-bromophenyl)anthracene (5.57 g) was obtained (the yield ratio: 95.1%).

DPyPA: 9,10-bis(3-bromophenyl)anthracene (5.36 g, 11.0 mmol), pyridine-3-boronic acid (3.10 g, 24 mmol), palladium chloride (PdCl₂, 0.266 g, 1.5 mmol), triphenyl phosphite (0.786 g, 3 mmol), potassium carbonate (12.4 g, 90 mmol), toluene (166 mL), ethyl alcohol (120 mL), and distilled water (153 mL) were added to a reaction flask under a nitrogen atmosphere. The reaction mixture was heated under reflux for five h before the organic fraction was isolated. The volatiles were removed in vacuo to leave a grey residue that was purified by column chromatography (silica gel) with petroleum ether/ethyl acetate (1:1) as eluent. A white solid (3.68 g, 76.0%) was obtained.

Spectroscopic characterization of DPyPA: ¹H NMR (600 MHz, 25 °C, CDCl₃, δ): 8.97 (s, 2H), 8.61 (d, $J = 7.2$ Hz, 2H), 7.97 (d, $J = 12.4$ Hz, 2H), 7.81 (s, 2H), 7.78–7.74 (m, 8H), 7.56 (t, $J = 10$ Hz, 2H), 7.39–7.37 (m, 6H); ¹³C-NMR (600 MHz, 25 °C, CDCl₃, δ): 148.81, 148.54, 134.54, 131.20, 129.97, 129.38, 126.96, 126.36, 125.44, 123.70; MS (EI): MW 484.59, m/z 484; elemental anal. calcd for (%): C, 89.23; H, 4.99; N, 5.78; found: C, 89.21; H, 5.01; N, 5.72; mp 276.7 °C.

Fabrication of OLEDs: ITO substrates with sheet resistance of 15 Ω/\square (square resistance) were sufficiently cleaned and treated with oxygen plasma before use. The EL devices were fabricated through vacuum deposition of the materials at 10^{-6} torr onto ITO glass. All the organic layers were deposited at a rate of 2.0 $\text{\AA} \text{ s}^{-1}$. The cathode was completed through thermal deposition of LiF at a deposition rate of 0.1 $\text{\AA} \text{ s}^{-1}$, and then capped with Al metal by thermal evaporation at a rate of 5.0 $\text{\AA} \text{ s}^{-1}$. The encapsulated device was characterized with a Keithley 4200 semiconductor characterization system in ambient conditions. The EL spectra were collected with a Photo Research PR705 spectrophotometer.

TOF Mobility Measurement: DPyPA was purified by sublimation before use in analyses and device fabrication. The TOF device was prepared by vacuum deposition using the following structure: ITO/Ag (60 nm)/DPyPA (1.4 μm)/Ag (200 nm). A third harmonic of the Nd:YAG laser (355 nm, 15 ns) is used as the excitation light source, which passes through the semitransparent electrode (Ag) and photogenerates a thin sheet of excess carriers. By switching the polarity of the applied dc bias, the transit time (T_t , the time that the carriers pass through the organic film to reach the counter electrode) is measured by a digital storage oscilloscope. With the applied bias V and the thickness, D , of the organic layer which is much greater than the optical absorption depth of the excitation, the carrier mobilities could be calculated according to the formula $\mu = D/(T_t E) = D^2/(VT_t)$.

Supporting Information

Supporting Information is available from the Wiley Online Library or from the author.

Table 1. Electroluminescent data of the devices.

| device parameter ^{a)} | Red OLEDs | | Green OLEDs | | Blue OLEDs | |
|--|----------------------|---------------------------------|----------------------|---------------------------------|----------------------|---------------------------------|
| | device A1 with DPyPA | device A2 with Alq ₃ | device B1 with DPyPA | device B2 with Alq ₃ | device C1 with DPyPA | device C2 with Alq ₃ |
| V _{on} [V] | 1.7 | 2.5 | 2.5 | 3.3 | 3.4 | 5.9 |
| V/V ^{b)} | 4.9 | 6.5 | 3.7 | 6.8 | 7.0 | 11.5 |
| η _c [cd A ⁻¹] ^{b)} | 5.98 | 3.89 | 21.69 | 17.19 | 11.26 | 7.63 |
| η _p [lm W ⁻¹] ^{b)} | 3.51 | 1.91 | 18.32 | 8.91 | 5.05 | 2.08 |
| η _{ext} [%] ^{b)} | 3.71 | 2.62 | 5.50 | 4.35 | 5.66 | 3.68 |
| λ _{em} [nm] | 608 | 608 | 520 | 520 | 472 | 472 |
| CIE(x, y) | (0.650, 0.349) | (0.648, 0.351) | (0.368, 0.612) | (0.375, 0.608) | (0.178, 0.337) | (0.175, 0.304) |
| L _{max} [cd m ⁻²] | 32112 | 18921 | 35667 | 35018 | 25950 | 21627 |
| η _{c, max} [cd A ⁻¹] | 6.22 | 4.11 | 22.52 | 17.52 | 12.31 | 8.23 |
| η _{p, max} [lm W ⁻¹] | 5.69 | 3.11 | 19.60 | 10.69 | 6.24 | 2.46 |
| η _{ext, max} [%] | 4.07 | 2.69 | 5.71 | 4.43 | 6.20 | 3.97 |

^{a)}Abbreviations: V_{on}: turn-on voltage; V: Voltage; L_{max}: maximum luminance; L: luminance; λ_{em}: emission wavelength; CIE(x,y): Commission International de l'Eclairage coordinates; η_{p, max}: maximum power efficiency; η_{c, max}: maximum current efficiency; η_{ext, max}: maximum external quantum efficiency; η_p: power efficiency; η_c: current efficiency; η_{ext}: external quantum efficiency; ^{b)}Data taken at the luminance 5000 cd m⁻².

Acknowledgements

We thank the National Natural Science Foundation of China (No. 50990060) and the National Key Basic Research and Development Program of China under Grant No. 2009CB623604 for support. Note: This article has been amended on May 24, 2011 to correct an error in Figure 6c of the version first published online.

Received: December 22, 2010
Published online: April 12, 2011

- [1] a) C. W. Tang, S. A. VanSlyke, *Appl. Phys. Lett.* **1987**, *51*, 913; b) J. H. Burroughes, D. D. C. Bradley, A. R. Brown, R. N. Marks, K. MacKay, R. H. Friend, P. L. Burn, A. B. Holmes, *Nature*, **1990**, *347*, 539; c) M. A. Baldo, D. F. O'Brien, Y. You, A. Shoustikov, S. Sibley, M. E. Thompson, S. R. Forrest, *Nature* **1998**, *395*, 151.
- [2] a) K. Katsuma, Y. Shirota, *Adv. Mater.* **1998**, *10*, 223; b) H. Tanaka, S. Tokito, Y. Taga, A. Okada, *Chem. Commun.* **1996**, 2175.
- [3] a) M. Uchida, T. Izumizawa, T. Nakano, S. Yamaguchi, K. Tamao, K. Furukawa, *Chem. Mater.* **2001**, *13*, 2680; b) S. Su, Y. Takahashi, T. Chibo, T. Takedo, J. Kido, *Adv. Funct. Mater.* **2009**, *19*, 1260.
- [4] H. Aziz, G. Xu, Z. D. Popovic, *Chem. Mater.* **2004**, *16*, 4522.
- [5] a) H. Sasabe, E. Gonmori, T. Chiba, Y.-J. Li, D. Tanaka, S.-J. Su, T. Takeda, Y.-J. Pu, K. Nakayama, J. Kido, *Chem. Mater.* **2008**, *20*, 5951; b) S.-J. Su, T. Chiba, T. Takeda, J. Kido, *Adv. Mater.* **2008**, *20*, 2125; c) K. Okumoto, H. Kanno, Y. Hamaa, H. Takahashi, K. Shibata, *Appl. Phys. Lett.* **2006**, *89*, 063504; d) H.-Y. Oh, C. Lee, S. Lee, *Org. Electron.* **2009**, *10*, 163; e) V. V. Jarikov, K. P. Klubek, L.-S. Liao, C. T. Brown, *J. Appl. Phys.* **2008**, *104*, 074914; f) V. V. Jarikov, *Appl. Phys. Lett.* **2008**, *92*, 244103; g) M. Ichikawa, T. Kawaguchi, K. Kobayashi, T. Miki, K. Furukawa, T. Koyama, Y. Taniguchi, *J. Mater. Chem.* **2006**, *16*, 221.
- [6] a) N. Miyaura, A. Suzuki, *Chem. Rev.* **1995**, *95*, 2457; b) R. Neeff, O. Bayer, *Chem. Ber.* **1957**, *90*, 1137; c) G. Li, H. Fang, S. Zhang, Z. Xi, *Tetrahedron Lett.* **2004**, *45*, 8399; d) H. Fang, C. Zhao, G. Li, Z. Xi, *Tetrahedron* **2003**, *59*, 3779; e) W. Cui, Y. Wu, H. Tian, Y. Geng, F. Wang, *Chem. Commun.* **2008**, *8*, 1017–1019.
- [7] a) Y. Shirota, N. Kinoshita, T. Noda, K. Okumoto, T. Ohara, *J. Am. Chem. Soc.* **2000**, *122*, 11021; b) P. G. Gassman, D. W. Macomber, J. W. Hershberger, *Organometallics* **1983**, *2*, 1470; c) S. Janietz, D. D. C. Bradley, M. Grell, C. Giebeler, M. Inbasekaran, E. P. Woo, *Appl. Phys. Lett.* **1998**, *73*, 2453.
- [8] a) R. G. Kepler, *Phys. Rev.* **1960**, *119*, 1226; b) Y.-L. Liao, C.-Y. Lin, Y.-H. Liu, K.-T. Wong, W.-Y. Hung, W.-J. Chen, *Chem. Commun.* **2007**, *18*, 1831.
- [9] B. Domercq, C. Grasso, J.-L. Maldonado, M. Halik, S. Barlow, S. R. Marder, B. Kippelen, *J. Phys. Chem. B* **2004**, *108*, 8647.
- [10] M. J. Frisch, G. W. Trucks, H. B. G. Schlegel, P. M. W. Gill, B. G. Johnson, M. A. Robb, J. R. Cheeseman, T. Keith, G. A. Petersson, J. A. Montgomery, K. Raghavachari, M. A. Al Laham, V. G. Zakrzewski, J. V. Ortiz, J. B. Foresman, J. Cioslowski, B. B. Stefanov, A. Nanayakkara, M. Challacombe, C. Y. Peng, P. Y. Ayala, W. Chen, M. W. Wong, J. L. Andres, E. S. Replogle, R. Gomperts, R. L. Martin, D. J. Fox, J. S. Binkley, D. J. Defrees, J. Baker, J. P. Stewart, M. Head-Gordon, C. Gonzalez, J. A. Pople, *Gaussian 09*, Revision A.9, Gaussian, Pittsburgh, PA **1998**.
- [11] a) A. D. Becke, *Phys. Rev. A* **1988**, *38*, 3098; b) C. Lee, W. T. Yang, R. G. Parr, *Phys. Rev. B* **1988**, *37*, 785; c) S. C. Tse, S. K. So, M. Y. Yeung, C. F. Lo, S. W. Wen, C. H. Chen, *Jpn. J. Appl. Phys.* **2006**, *45*, 555.
- [12] a) P. Wei, L. Duan, D. Zhang, J. Qiao, L. Wang, R. Wang, G. Dong, Y. Qiu, *J. Mater. Chem.* **2008**, *18*, 806; b) Y. Sun, L. Duan, P. Wei, J. Qiao, G. Dong, L. Wang, Y. Qiu, *Org. Lett.* **2008**, *11*, 2069.
- [13] a) Q.-X. Tong, S.-L. Lai, M.-Y. Chan, Y.-C. Zhou, H.-L. Kwong, S.-T. Kwon, O. Kwon, *J. Phys. Chem. C* **2009**, *113*, 6227; b) L.-Z. Yu, X.-Y. Jiang, Z.-L. Zhang, L.-R. Lou, C.-T. Lee, *J. Appl. Phys.* **2009**, *105*, 013105; c) X.-Y. Jiang, Z.-L. Zhang, W.-Q. Zhu, S.-H. Xu, *J. Phys. D: Appl. Phys.* **2005**, *38*, 4153; d) J. D. Debad, P. Magnus, A. J. Bard et al. *J. Org. Chem.* **1997**, *62*, 530; e) S. J. Woo, J. P. Tae, H. K. Jang, *Mol. Cryst. Liq. Cryst.* **2009**, *513*, 227.
- [14] T. Oyamada, H. Yoshizaki, C. Adachi, *Chem. Lett.* **2004**, 1034.
- [15] a) C. Féry, B. Racine, D. Vaufrey, H. Doyeux, S. Cinà, *Appl. Phys. Lett.* **2005**, *87*, 213502; b) L. S. Liao, W. K. Slusarek, T. K. Hatwar, M. L. Ricks, D. L. Comfort, *Adv. Mater.* **2008**, *20*, 324.
- [16] H. Doi, M. Kinoshita, K. Okumoto, Y. Shirota, *Chem. Mater.* **2003**, *15*, 1080.